

Improved Stability Regions for Ground States of the Extended Hubbard Model

Zsolt Szabó

Institut für Theoretische Physik, Universität zu Köln, Zülpicher Str. 77, D-50937 Köln, Germany
(6 July 1998)

In the present paper certain sectors of the ground state phase diagram of the extended Hubbard model containing nearest and next-nearest neighbor interactions have been investigated using an exact method in the thermodynamic limit. It is found that the inclusion of further local correlations and of next-nearest neighbor interactions both have significant effects on the position of the phase boundaries. Improved stability domains for the η -pairing state and for the fully saturated ferromagnetic state at half filling have been constructed. The results prove these states to be the ground states for model Hamiltonians with realistic values of the interaction parameters.

PACS number: 74.20.-z, 75.10.Jm, 75.10.Lp

I. INTRODUCTION

Exact solutions in physics are of great importance since the approximations used in studying a special phenomenon can dominate the deduced results so extremely that one might end up with a totally incorrect description of the studied phenomenon itself. Applying an analytic, nevertheless non-exact, approach one always has to have of precise knowledge of the extent to which the approximation is valid. In case of methods based on perturbation theory, this means e.g., that a well-defined, *small* parameter should be found in order to be sure that higher order terms are really negligible. Often, it is extremely difficult to find this small parameter. This is due to the fact that the given phenomenon itself has strong-coupling characteristics and the associated correlation effects are non-negligible at all. This is especially true for the investigation of features of strongly correlated electron systems. Ferromagnetism is one example, which is an *intermediate to strong* coupling phenomenon. One has to be cautious when applying a perturbative approach to this problem.

Considering the exact results with respect to the dimensionality D , most of them have been derived in two limiting cases: either in $D=1$ or in $D=\infty$. As an example the Hubbard model is cited here, the exact solution of which was given in $D=1$ dimension by means of the Bethe-ansatz by Lieb and Wu¹. The other class of exact solutions belongs to the other limiting case, that of $D=\infty$, where the dynamical mean-field approximation becomes exact^{2,3}. The situation, however, gets more complicated as physically existing, lower dimensional cases (e.g. systems in $D=2$ or $D=3$ dimensions) are considered. $D > 1$ rules out the applicability of the well-established Bethe-ansatz approach, while mean-field like descriptions lead to qualitatively incorrect conclusions as the effects of fluctuations are not taken into account properly^{4,5}.

In recent years a few exact, *non-perturbative*, methods have been developed, by means of which the ground state of Hubbard and Hubbard-like models can be investigated in large parameter regimes^{6–13}. In the present work we choose to focus mainly on the so-called optimal ground state method (OGS) established by de Boer and Schadschneider¹². Using this method one can easily deduce some rigorous constraints for the model parameters. If these are satisfied e.g. the CDW, the Néel, the fully saturated ferromagnetic or the η -pairing states of momentum P become exact ground states of the Hamiltonian.

As far as the OGS method is concerned, the basic idea is to diagonalize a specially chosen local Hamiltonian and to make all the local eigenstates which are needed for the construction of a given global ground state also local ground states. This means on the one hand, that the corresponding eigenvalues of the local Hamiltonian should be all equal in magnitude and on the other hand, this common value should be the lowest eigenvalue of the local problem. Following this line, one can obtain different regions for different many particle states in the parameter space of the model defined by inequalities. The inequalities mean *sufficient* conditions for a state to be the ground state inside a special region. Outside the derived region the state under study can still be the ground state of the model.

There are basically two different ways to enlarge the region of guaranteed stability, namely the choice of a larger local Hamiltonian or the incorporation of next-nearest neighbor interactions. As far as the first approach is concerned, it is obvious that the extent of local correlations taken into account is controlled by the size of the local Hamiltonian that is exactly diagonalized. Therefore, the usage of local Hamiltonians defined on larger clusters of the lattice should typically lead to better constraints (extended stability regions), even if purely nearest neighbor interactions are included.

It is also a well-established fact, that the inclusion of next-nearest neighbor interactions has important effects. For instance, it was shown rigorously by Tasaki¹⁴, that the pure Hubbard model characterized by hopping of electrons

between nearest and next-nearest neighboring sites with dispersive bands exhibits ferromagnetism for finite Coulomb interaction at zero temperature. Recent Projection Quantum Monte Carlo studies by Hlubina *et al.*¹⁵ confirmed this fact for finite temperatures, too. Beside the consequences of longer range hopping, the importance of nearest and next-nearest neighbor off-site interactions (diagonal and off-diagonal) has also been emphasized both from experimental¹⁶ and theoretical^{4,10,11,17,18} side. These extra terms (density-density type interaction, correlated hopping of electrons, hopping of pairs of electrons and the exchange coupling) all originate from the spin independent Coulomb interaction of electrons in solids. Nevertheless, the values of these longer range interactions (e.g. between electrons associated to next-nearest neighboring sites) are known neither theoretically nor experimentally because the screening processes in solids are not known precisely enough. But it is obvious that these interactions are present in real materials. Their values decrease for increasing interatomic distances in the lattice and they can have important consequences on the characteristics of strongly correlated electron systems. Hence, it is a challenging task to incorporate and treat them in an exact fashion on the level of the model Hamiltonian.

The aim of the present paper is hence two-fold. We would like to show the consequences of a specially chosen larger local Hamiltonian defined on elementary plaquettes consisting of four lattice sites of the D dimensional hypercubic lattice extending the previous calculations¹². Using these local Hamiltonians and a simple, numerically exact method we have constructed the stability domains for the η -pairing states of momentum $P = 0, \pi$ and for the fully saturated ferromagnetic state in the parameter space of an extended Hubbard model with a half-filled band. Since the analytic diagonalization of the local Hamiltonian is quite difficult, the diagonalization is done numerically. The stability regions are deduced from the equality of the lowest eigenvalue of the chosen local Hamiltonian and of an upper bound derived appropriately in terms of the variational principle of quantum mechanics. This states that the ground state energy of a given Hamiltonian can always be bounded from above by the expectation value of the Hamiltonian calculated by means of a variational wavefunction. The present choice of the larger local Hamiltonian also enables us to incorporate the next-nearest neighbor interactions in a simple way.

The present paper is organized as follows: in Sec. II we introduce the applied method. In Sec. III the global and the corresponding local Hamiltonians are defined. Sections IV A and IV B contain the stability domains in $D = 2, 3$ for the η -pairing states of momentum P and for the fully saturated ferromagnetic case, respectively. Finally a short summary with discussion closes the presentation in Sec. V.

II. METHOD

Let us consider a model Hamiltonian defined on a lattice. Each, so-called global Hamiltonian, can be decomposed into the sum of totally equivalent local Hamiltonians defined on smaller clusters of the lattice. So the equation

$$H = \sum_{\text{all clusters}} h_{\text{cluster}} \quad (1)$$

always holds. If we concentrate, for example, only on completely local effects, the clusters are simply the local Hamiltonians defined at the individual lattice points. If intersite effects should also be incorporated the proper *minimal* local Hamiltonian is actually a bond Hamiltonian concerning two lattice sites. Nevertheless, the incorporation of longer and longer range interactions, or of more and more correlations, requires the enlargement of the minimal cluster. In principle, interactions and correlations can be taken into account up to infinite range. But this requires the choice of $h_{\text{cluster}} = H$. The tractable cluster size is, however, limited by the feasibility of the necessary exact diagonalization.

Setting up the local Hamiltonian and choosing a suitable local basis, on the one hand, the eigenvalue problem

$$h_{\text{cluster}} |\phi_{\text{cluster}}\rangle = \epsilon_{\text{cluster}} |\phi_{\text{cluster}}\rangle \quad (2)$$

can be solved exactly. Thus the whole spectrum $\epsilon_{\text{cluster}}^i$ ($i = 1, \dots, \dim(h_{\text{cluster}})$) of h_{cluster} can be obtained. Since the blocks of decomposition are totally equivalent, the exact ground state energy E_{GS} can be bounded from below by the relation

$$E_{\text{lower}} = N_{\text{cluster}} \min_i \epsilon_{\text{cluster}}^i \leq E_{\text{GS}} , \quad (3)$$

where the number of clusters on the considered lattice can be determined as $N_{\text{cluster}} = fL$. Here f represents a simple combinatorical factor depending on the dimension and structure of the underlying lattice and L stands for the number of lattice sites.

On the other hand, the variational principle of quantum mechanics provides an upper bound for E_{GS} , namely

$$E_{\text{GS}} \leq \frac{\langle \Psi_{\text{trial}} | H | \Psi_{\text{trial}} \rangle}{\langle \Psi_{\text{trial}} | \Psi_{\text{trial}} \rangle} = E_{\text{upper}} , \quad (4)$$

where $|\Psi_{\text{trial}}\rangle$ stands for an arbitrary trial wavefunction. In our case $|\Psi_{\text{trial}}\rangle$ is an exact eigenstate of the global Hamiltonian for a certain set of model parameters.

Combining now Eqs. (3,4), we get the following inequality among E_{lower} , E_{GS} and E_{upper} ,

$$E_{\text{lower}} \leq E_{\text{GS}} \leq E_{\text{upper}} . \quad (5)$$

Exploiting now the fact, that both E_{lower} and E_{upper} are analytic functions of the couplings in the global Hamiltonian, after carefully adjusting the coupling constants one can satisfy the equality

$$E_{\text{lower}} = E_{\text{upper}} \equiv E_{\text{GS}} , \quad (6)$$

which means that for a certain set of model parameters (in a special sector of the ground state phase diagram) the exact ground state energy E_{GS} is found. Furthermore, if the ground state has no degeneracy, the exact ground state $|\Psi_{\text{GS}}\rangle$ of the global Hamiltonian is also found. In our case the non-degeneracy is provided by the fact, that the considered states (see Sec. IV) can be built up simply by using the lowest energy eigenstates of the local Hamiltonian. As an example let us consider the case of the $D=1$ dimensional half-filled chain, with bonds as clusters. In principle, it can be reached for certain values of the coupling constants that the non-degenerate lowest eigenvalue of the local Hamiltonian belongs to the parallel orientation of spins included in the bond. Since the bonds are equivalent, all the bonds along the chain have parallel-oriented spins with the same local energy for this set of model parameters. This fact yields the long range order of spins (here ferromagnetism) on the level of the chain and also the non-degeneracy of the global ground state. Similar argumentation holds for the non-degeneracy of different ground states in higher dimensions, too.

Changing now the trial wavefunction and following the above discussed procedure, a new ground state in a different region of the phase diagram can be verified. Furthermore, repeating the method with more and more trial wavefunctions, a large portion of the ground state phase diagram of the model under study can be explored.

III. GLOBAL AND LOCAL HAMILTONIAN

Let us define now our global Hamiltonian on a D dimensional hypercubic lattice ($D > 1$) in the following form

$$H = \sum_{i,j} \left[-t_{ij} \hat{t}_{ij} + X_{ij} \hat{X}_{ij} + U_{ij} \hat{U}_{ij} + Y_{ij} \hat{Y}_{ij} + J_{ij} \hat{J}_{ij} \right] - \mu \hat{\mu} , \quad (7)$$

where

$$\begin{aligned} \hat{t}_{ij} &= \sum_{\sigma} c_{i\sigma}^{\dagger} c_{j\sigma} \\ \hat{X}_{ij} &= \sum_{\sigma} c_{i\sigma}^{\dagger} c_{j\sigma} (n_{i,-\sigma} + n_{j,-\sigma}) \\ \hat{U}_{ij} &= \frac{1}{2} \sum_{\sigma, \sigma'} n_{i\sigma} n_{j\sigma'} \\ \hat{Y}_{ij} &= c_{i\uparrow}^{\dagger} c_{i\downarrow}^{\dagger} c_{j\downarrow} c_{j\uparrow} \\ \hat{J}_{ij} &= \Delta_{ij}^{XY} (S_i^x S_j^x + S_i^y S_j^y) + \Delta_{ij}^Z S_i^z S_j^z \\ \hat{\mu} &= \sum_{i,\sigma} n_{i\sigma} . \end{aligned}$$

Here the fermion operators $c_{i\sigma}^{\dagger}$ and $c_{i\sigma}$ create and annihilate, respectively, electrons with spin σ in the single tight-binding Wannier orbital associated with site i , $n_{i\sigma}$ is the particle number operator, \vec{S}_i is a Heisenberg spin with components (S_i^x, S_i^y, S_i^z) . The above Hamiltonian contains a term corresponding to the hopping of a single electron (characterized by t_{ij}), a density dependent (or correlated) hopping term (X_{ij}), two-particle density-density type interactions of electrons (U_{ij}), a term describing the hopping of pairs of electrons (Y_{ij}), for $\Delta_{ij}^{XY} = \Delta_{ij}^Z = 1$ a Heisenberg-type exchange interactions of local spins (J_{ij}) and a chemical potential term (μ). We briefly note here, that

$\Delta_{ij}^{XY} = 0$, $\Delta_{ij}^Z = 1$ represents an Ising-type coupling of local spins, while the case of $\Delta_{ij}^{XY} = 1$, $\Delta_{ij}^Z = 0$ corresponds to an XY-type interaction of these. $J_{ij} > 0$ ($J_{ij} < 0$) corresponds to the antiferromagnetic (ferromagnetic) type of exchange interaction of the spins. The relevance of the present model for real materials is discussed e.g. in^{4,20}.

In what follows we are interested only in couplings between on-site, nearest-neighbor and next-nearest neighbor electrons. Incorporating this restriction into Eq. (7) and using the convention $A_l = A_{ij}$ ($l = 1, 2$ for i, j being nearest, next-nearest neighboring sites, respectively) for the intersite couplings, one can rewrite the global Hamiltonian as

$$H = U \sum_{i=1}^L \left(n_{i\uparrow} - \frac{1}{2} \right) \left(n_{i\downarrow} - \frac{1}{2} \right) + \sum_{l=1}^2 \sum_{\langle ij \rangle_l} \left\{ \frac{1}{2} \sum_{\sigma} [X_l(n_{i,-\sigma} + n_{j,-\sigma}) - t_l] (c_{i\sigma}^{\dagger} c_{j\sigma} + c_{j\sigma}^{\dagger} c_{i\sigma}) + \frac{1}{2} V_l(n_i - 1)(n_j - 1) + \frac{1}{2} Y_l (c_{i\uparrow}^{\dagger} c_{i\downarrow}^{\dagger} c_{j\downarrow} c_{j\uparrow} + c_{j\uparrow}^{\dagger} c_{j\downarrow}^{\dagger} c_{i\downarrow} c_{i\uparrow}) + \frac{1}{2} J_{xy}^{(l)} (S_i^+ S_j^- + S_j^+ S_i^-) + J_z^{(l)} S_i^z S_j^z \right\} - \mu \hat{\mu} - E_0, \quad (8)$$

with $n_i = n_{i\uparrow} + n_{i\downarrow}$, $S_i^z = \frac{1}{2}(n_{i\uparrow} - n_{i\downarrow})$, $S_i^+ = c_{i\uparrow}^{\dagger} c_{i\downarrow}$ and $S_i^- = c_{i\downarrow}^{\dagger} c_{i\uparrow}$. Here $\langle ij \rangle_l$ means the l th neighboring sites. In the following the new notations $J_{xy}^{(l)} = \Delta_l^{XY} J_l$ and $J_z^{(l)} = \Delta_l^Z J_l$ are also used. In the special case of $\Delta_i^{XY} = \Delta_l^Z = 1$, however, the $J_l \equiv J_{xy}^{(l)} = J_z^{(l)}$ notation will be kept for the sake of clarity. E_0 represents a numerical constant which shifts the zero point of the energy scale. We mention here, that during the reformulation of (7) to (8) the chemical potential is also shifted by some constant.

Because of the inclusion of interactions only between electrons situated on nearest and next-nearest neighboring sites the minimal clusters, which are fully symmetric, are the two-dimensional elementary plaquettes of the $D=2$ dimensional square lattice, as depicted in Fig. 1. All the $D > 2$ dimensional hypercubic lattices can be covered with the elementary plaquettes, however, in those cases the D dimensional hypercubes would be the fully symmetric minimal clusters. Following the method of Sec. II, the global Hamiltonian can be rewritten in terms of such plaquettes ($\sum_{[i,j,l,m]}$ means a summation over the different plaquettes), as

$$H = \sum_{[i,j,l,m]} h_{ijlm} \quad (9)$$

with

$$h_{ijlm} = \frac{U}{z_2} \sum_{\alpha \in \mathcal{A}_0} \left(n_{\alpha\uparrow} - \frac{1}{2} \right) \left(n_{\alpha\downarrow} - \frac{1}{2} \right) + \frac{X_1}{4f_1} \sum_{(\alpha,\beta) \in \mathcal{A}_N} \sum_{\sigma} (c_{\alpha,\sigma}^{\dagger} c_{\beta,\sigma} + c_{\beta,\sigma}^{\dagger} c_{\alpha,\sigma}) (n_{\alpha,-\sigma} + n_{\beta,-\sigma}) + \frac{X_2}{f_2} \sum_{(\alpha,\beta) \in \mathcal{A}_{NN}} \sum_{\sigma} (c_{\alpha,\sigma}^{\dagger} c_{\beta,\sigma} + c_{\beta,\sigma}^{\dagger} c_{\alpha,\sigma}) (n_{\alpha,-\sigma} + n_{\beta,-\sigma}) - \frac{t_1}{4f_1} \sum_{(\alpha,\beta) \in \mathcal{A}_N} \sum_{\sigma} (c_{\alpha,\sigma}^{\dagger} c_{\beta,\sigma} + c_{\beta,\sigma}^{\dagger} c_{\alpha,\sigma}) - \frac{t_2}{f_2} \sum_{(\alpha,\beta) \in \mathcal{A}_{NN}} \sum_{\sigma} (c_{\alpha,\sigma}^{\dagger} c_{\beta,\sigma} + c_{\beta,\sigma}^{\dagger} c_{\alpha,\sigma}) + \frac{V_1}{4f_1} \sum_{(\alpha,\beta) \in \mathcal{A}_N} (n_{\alpha} - 1)(n_{\beta} - 1) + \frac{V_2}{f_2} \sum_{(\alpha,\beta) \in \mathcal{A}_{NN}} (n_{\alpha} - 1)(n_{\beta} - 1) + \frac{Y_1}{4f_1} \sum_{(\alpha,\beta) \in \mathcal{A}_N} (c_{\alpha\uparrow}^{\dagger} c_{\alpha\downarrow}^{\dagger} c_{\beta\downarrow} c_{\beta\uparrow} + c_{\beta\uparrow}^{\dagger} c_{\beta\downarrow}^{\dagger} c_{\alpha\downarrow} c_{\alpha\uparrow}) + \frac{Y_2}{f_2} \sum_{(\alpha,\beta) \in \mathcal{A}_{NN}} (c_{\alpha\uparrow}^{\dagger} c_{\alpha\downarrow}^{\dagger} c_{\beta\downarrow} c_{\beta\uparrow} + c_{\beta\uparrow}^{\dagger} c_{\beta\downarrow}^{\dagger} c_{\alpha\downarrow} c_{\alpha\uparrow}) + \frac{J_{xy}^{(1)}}{4f_1} \sum_{(\alpha,\beta) \in \mathcal{A}_N} (S_{\alpha}^+ S_{\beta}^- + S_{\beta}^+ S_{\alpha}^-) + \frac{J_{xy}^{(2)}}{f_2} \sum_{(\alpha,\beta) \in \mathcal{A}_{NN}} (S_{\alpha}^+ S_{\beta}^- + S_{\beta}^+ S_{\alpha}^-) + \frac{J_z^{(1)}}{2f_1} \sum_{(\alpha,\beta) \in \mathcal{A}_N} S_{\alpha}^z S_{\beta}^z + J_z^{(2)} \sum_{(\alpha,\beta) \in \mathcal{A}_{NN}} S_{\alpha}^z S_{\beta}^z - \frac{\mu}{z_2} \sum_{\alpha \in \mathcal{A}_0} n_{\alpha} \quad (10)$$

Here $f_1 = z_2/z_1$ and $f_2 = 2$ ($z_1 = 2D$ and $z_2 = 4\binom{D}{2}$ are the number of nearest and next-nearest neighboring sites, respectively, on the D dimensional hypercubic lattice) are numerical constants. They are needed to avoid double or

higher counting of intersite interactions during the plaquette summation. Furthermore, t_1, X_1, V_1, Y_1 are the values of single electron hopping, correlated hopping, density-density type interaction and pair-hopping between nearest neighboring sites, respectively, while t_2, X_2, V_2, Y_2 indicate the analogous processes between next-nearest neighboring sites. U is the Hubbard interaction which can be either positive or negative at the level of the model. To mimic real systems, however, it should be repulsive. In addition, spin interactions with exchange couplings $J_{xy}^{(1)}, J_{xy}^{(2)}, J_z^{(1)}$ and $J_z^{(2)}$ are included on the plaquette. Further notations are: $\mathcal{A}_0 = \{i, j, l, m\}$ means the set of individual lattice points, $\mathcal{A}_N = \{(i, j), (j, l), (l, m), (m, i)\}$ represents the set of nearest neighboring sites and $\mathcal{A}_{NN} = \{(i, l), (j, m)\}$ indicates the set of next-nearest neighboring sites in the plaquette (see Fig. 1). The possibility of anisotropies can be naturally incorporated into the local (and hence global) Hamiltonian via the non-equivalence of the orthogonal directions of the plaquette. The effects of anisotropies, however, are not discussed in the present paper.

To apply Eq. (6), the connection between the number of lattice sites L and the number of clusters N_{cluster} (here plaquettes) should also be known. For this, combinatoric considerations give the following simple result on a D dimensional hypercubic lattice, namely

$$N_{\text{cluster}} = \frac{1}{2} D(D-1)L \quad (11)$$

IV. RESULTS

As an illustration of the method described in Sec. II, in what follows we consider two physically interesting states, the η -pairing states of momentum P (further explanation see below in Sec. IV A) which show off-diagonal long range order and are hence superconducting and the fully saturated ferromagnetic state (Sec. IV B). We try to determine under what circumstances these states are the ground states of (7). All the calculations presented are done at half filling. Except for the η -pairing states of momentum $P = 0$, it is not possible to express the results in a compact analytic form as it has been done earlier in Ref.¹². Therefore and for the sake of visualization we have restricted ourselves to special cuts of the parameter space to illustrate the effects of the larger local Hamiltonian and of next-nearest neighbor couplings. The cuts are chosen in such a way, that the corresponding ground state phase diagrams can be easily compared with the previously published rigorous results of Strack *et al.*¹¹, de Boer *et al.*^{12,24} and Montorsi *et al.*²⁵. In principle, one can also investigate the role of all the various nearest and next-nearest terms separately, one by one, using the above method.

A. η -pairing states of momentum P

As a short reminder, the definition of the η -pairing operator of momentum P is given by the relation

$$\eta_P^\dagger = \sum_{j=1}^L e^{iPj} c_{j\downarrow}^\dagger c_{j\uparrow}^\dagger. \quad (12)$$

Using this operator an η -pairing state of momentum P and of pairs N can easily be constructed via the relation

$$|\Psi_\eta(N, P)\rangle = K \left(\eta_P^\dagger \right)^N |0\rangle, \quad (13)$$

where $K = \left[\frac{(L-N)!}{L! N!} \right]^{\frac{1}{2}}$ is a normalization factor. For further details about the η -pairing states the reader is referred to the literature^{21–25}. Since we would like the η -pairing states to be the ground state of our model, it is instructive to calculate the commutator of the η -operator with the global Hamiltonian (7). After a trivial, but tedious computation one finds that

$$\begin{aligned} [H, \eta_P^\dagger] &= \sum_{k=1}^2 \left[\frac{1}{2} (X_k - t_k) \sum_{\langle jl \rangle_k} (e^{iPj} + e^{iPl}) (c_{j\downarrow}^\dagger c_{l\uparrow}^\dagger + c_{l\downarrow}^\dagger c_{j\uparrow}^\dagger) \right. \\ &\quad \left. + \frac{1}{2} X_k \sum_{\langle jl \rangle_k} (e^{iPj} - e^{iPl}) \left[(n_{l\uparrow} - n_{j\downarrow}) c_{l\downarrow}^\dagger c_{j\uparrow}^\dagger + (n_{l\downarrow} - n_{j\uparrow}) c_{j\downarrow}^\dagger c_{l\uparrow}^\dagger \right] \right] \end{aligned}$$

$$\begin{aligned}
& + \sum_{\langle jl \rangle_k} \left\{ \left(\frac{1}{2} Y_k e^{iPj} - U_k e^{iPl} \right) (n_j - 1) c_{l\uparrow}^\dagger c_{l\downarrow}^\dagger \right. \\
& \quad \left. + \left(\frac{1}{2} Y_k e^{iPl} - U_k e^{iPj} \right) (n_l - 1) c_{j\uparrow}^\dagger c_{j\downarrow}^\dagger \right\} \Big] - 2\mu\eta_P^\dagger
\end{aligned} \tag{14}$$

Calculating now $[H, (\eta_P^\dagger)^N] |0\rangle$, one can easily deduce the constraints in order that the η -pairing states of momentum P be the ground state of the starting model; for momentum $P = 0$ one comes to the requirements $X_i = t_i$ and $Y_i = 2V_i$ ($i=1,2$), while for momentum $P = \pi$ the conditions $X_2 = t_2$ and $Y_i = (-1)^i 2V_i$ ($i=1,2$) should be satisfied. One would also look at η -pairing states of momentum $P \neq 0$ or π . But they represent the ground states of model (7), where $X_i = t_i$ ($i=1,2$), $U \leq -4t_1$ with all the other interaction constants being zero^{26,27}.

Using the η -pairing states as trial wavefunctions, the upper bound in the thermodynamic limit for the ground state energy per lattice site L is

$$\frac{E_{\text{upper}}^{\eta_P}}{L} = \frac{1}{4}(U + z_1 V_1 + z_2 V_2) + \frac{1}{2}n\left(\frac{1}{2}n - 1\right) \sum_{l=1}^2 z_l V_l + \frac{1}{4}n\left(1 - \frac{1}{2}n\right) \sum_{l=1}^2 z_l Y_l \cos^l P - \mu n \tag{15}$$

or at half filling ($n = 1$), exploiting the constraints between the amplitudes of pair-hopping Y_i and that of density-density type interaction V_i one gets

$$E_{\text{upper}}^{\eta_P} = \frac{1}{4}L \left(U + \sum_{l=1}^2 z_l V_l \right) - \mu L. \tag{16}$$

Despite the fact, that the upper bounds are the same for η -pairing states of momentum $P = 0$ or π , there is a characteristic difference between the two sets of wavefunctions; the state $|\Psi_\eta(N, P=\pi)\rangle$ remains an exact eigenstate of (7) even if $X_1 \neq t_1$ holds.

As it was mentioned earlier, using larger local Hamiltonians it is possible to include more correlations which preferably lead to the extension of the stability of a chosen state and hence to improved phase boundaries. This effect for the η -pairing state of momentum $P = 0$ is depicted in Fig. 2, choosing the special \tilde{J}_{xy} - \tilde{J}_z cut of the coupling constants' space: the inner triangle corresponds to the stability domain of η_0 -state applying the OGS method of de Boer *et al.*¹² with bonds as local Hamiltonians while the shaded regions give the improvements of these boundaries on taking plaquette Hamiltonians containing purely nearest neighbor interactions into consideration. The axis $\tilde{J}_a = J_a^{(1)} A(U, V_1, V_2 = 0)$ ($a = xy, z$) represent the rescaled values of the nearest neighbor (Heisenberg) spin exchange interactions with the scaling factor of

$$A(U, V_1, V_2) = \left[2 \frac{z_2}{z_1} \left| \frac{U}{2z_2} + V_1 + V_2 \right| \right]^{-1}. \tag{17}$$

From the figure one can immediately read off the stability criteria for η_0 being the ground state of (7) in the absence of next-nearest neighbor hopping, correlated hopping and exchange interactions ($t_2 = X_2 = J_2 = 0$) for $V_1 \leq 0$ values of the nearest neighbor density-density type interaction, that is

$$\begin{aligned}
V_1 & \leq 0 \\
-t_1^2 & \leq \tilde{J}_z t_1 \leq -2\tilde{J}_{xy}^2 + t_1^2,
\end{aligned} \tag{18}$$

which is a considerable improvement over the $V_1 \leq 0$, $-t_1^2 \leq \tilde{J}_z t_1 \leq -2|\tilde{J}_{xy}| + t_1^2$ criteria following the line of¹² using bond Hamiltonians.

In real systems, the $X_1 = t_1$ requirement does not hold in general. But the values of the corresponding two interactions are of the same magnitude. For $X_1 \neq t_1$ only the η -pairing state of momentum $P = \pi$ represents an exact eigenstate of the model Hamiltonian. Figure 3 shows the stability regions for the η_π -state as ground state in the U - t_1 plane for two different set of model parameters in units of eV . The dotted lines represent the boundary for stability regions derived by the use of bond Hamiltonians while the solid lines are the boundaries calculated with the usage of plaquette Hamiltonians in the absence of next-nearest neighbor interactions. The shaded regions clearly show the extension of stability regions due to the choice of larger local Hamiltonians.

We now consider the phase diagrams in the U - V_1 (Fig. 4) and V_2 - V_1 (Fig. 5) planes for fixed values of the remaining interactions. For Fig. 4 the exchange interaction has been fixed by the relation $J_1 = -2Y_1$, which assures that the global Hamiltonian of Sec. III coincides with the model Hamiltonian of²⁵, where the authors derived rigorous bounds

for the η_π -state using the method of positive definite operators^{8,10,11}. Comparing Fig. 4 with Fig. 1 of that work, two basic differences can be realized. First, the boundary of the stability region, even for the special case of $X_1 = t_1$, varies with increasing values of nearest neighbor pair-hopping amplitude Y_1 and has a maximum at $Y_1 \approx 1.33t_1$ instead of having a constant value. Second, the value of this maximum $U_{max} \approx -0.33z_1t_1$ is independent of X_1 . Furthermore, for all values of X_1/t_1 the stability regions derived with the present method are always larger than the corresponding ones predicted by Montorsi *et al.*²⁵ and de Boer *et al.*¹² and exist for all positive values of Y_1 . Since the $Y_1 = -2V_1$ requirement, originating from the fact that the η_π -state has to be an exact eigenstate of the model under study, should also be satisfied, the observation concerning the positivity of Y_1 implies that the nearest neighbor density-density type interaction V_1 should be always negative, i.e. attractive.

As the η -pairing states consist of local pairs of electrons, it is of interest to investigate the effects of on-site Coulomb repulsion, characterized by U , on the stability of these pairs. To shed light on this issue, we considered the V_2 - V_1 plane for various values of U . As can be seen in Fig. 5, the local pairs can be stable in the presence of even relatively large positive values of U . This requires, however, definitely an attraction in the nearest neighbor density-density interaction channel. It should be noted also, that the same type of interaction between next-nearest neighbors, V_2 , can either be attractive or moderately repulsive. These findings lead us to the conclusion, that the η -pairing states of momentum $P = \pi$ remain the ground states of (7) even for positive values of the on-site Coulomb interaction. Hence, superconductivity can exist in the extended Hubbard model in the case of local repulsion, if a sufficiently strong nearest neighbor attraction is present.

The inclusion of next-nearest neighbor interactions increases remarkably the number of model parameters and hence the number of possible cuts of the parameter space. Therefore, we try to illustrate only some special, overall effects of these interactions in the followings. In order to be close to real systems, all the next-nearest neighbor interactions are chosen in such a way, that they are smaller in magnitude than the corresponding nearest neighbor ones. But the ratios of nearest to next-nearest neighbor interactions can be very different; they depend on the material. In Fig. 6 three plots are shown for different values of the couplings. These results are found in $D = 2$, the corresponding 3-dimensional plots display qualitatively the same features, except for the parameters of Fig. 6c. The discrepancy between the plots taken in $D = 2$ and $D = 3$ is due to the fact that the number of next-nearest neighbors z_2 is much larger in $D = 3$ than in $D = 2$, $z_2(D = 3)/z_2(D = 2) = 3$. This suggests that the effects of next-nearest neighbor interactions in the framework of the present model might be stronger in higher dimensions.

In Fig. 6a the stability region of the η -pairing state of momentum $P = 0$ is shown for a certain set of model parameters in the absence (solid line) and in the presence (dotted line) of next-nearest neighbor couplings. One can immediately notice the expansion of the stability region due to the presence of next-nearest neighbor interactions. For large values of $|t_1|$, however, the size of the stability region shrinks. This is due to the fact that a large value of nearest neighbor hopping (in the presence of a fixed value of Y_1) favors the hopping of single electrons instead of the hopping of pairs of electrons, and hence gives rise to the breaking of local pairs. This means that the number of doubly occupied sites does not conserve any longer. The consequence of the pair breaking is, that the η_0 -state ceases to be the ground state of (7). In Fig. 6b the effects of next-nearest neighbor interactions on the stability of the η_π -state are considered. In contrast to the situation depicted in Fig. 6a no shrinking of the stability domain with increasing $|t_1|$ can be observed. This finding can be explained with the different internal structure of the η_π pairs. With Fig. 6c we would like to illustrate a situation where next-nearest neighbor couplings can either increase or decrease the stability region of the η_π -state depending on their actual numerical values. As mentioned earlier, the dimension of the lattice plays a crucial role here; in $D = 2$ a huge portion of the U - Y_1 phase diagram is occupied by the η_π -state for any ratio of X_1/t_1 . In $D = 3$, however, it was found in a wide parameter region that the η_π -state is the ground state only for the special case of $X_1/t_1 = 1$.

B. The fully polarized ferromagnetic state

Let us consider now the fully polarized ferromagnetic state as the trial wave function defined by

$$|\Psi_{FM}\rangle = \prod_{j=1}^L c_{j\uparrow}^\dagger |0\rangle = \hat{F}|0\rangle. \quad (19)$$

Calculating the commutator of \hat{F} with Hamiltonian (7) one can see that the fully polarized ferromagnetic state is an exact eigenstate of the global Hamiltonian for any values of the interaction parameters. The trial wavefunction $|\Psi_{FM}\rangle$ yields in the thermodynamic limit at half-filling the upper bound

$$E_{\text{upper}}^{\text{FM}} = -\frac{1}{4}UL + \frac{1}{8}L \sum_{l=1}^2 z_l J_z^{(l)} - \mu L \quad (20)$$

for the ground state energy.

In what follows, we try to reveal under what circumstances (19) is the ground state of the Hamiltonian (7). For the sake of simplicity we concentrate on a fixed, realistic set of values regarding the nearest neighbor couplings which have already been estimated by Hubbard²⁸ for electrons in d -bands of transition metals. Concerning the values of next-nearest neighbor interactions, they are chosen to be fractions of the corresponding nearest neighbor ones. The ratio of nearest to next-nearest neighbor couplings is chosen to be about 5-8. We believe this range of ratio to be appropriate for a wide class of materials. Furthermore, this is in agreement with the work of Appel *et al.*²⁹ who made quantitative predictions for the values of nearest and next-nearest neighbor correlated hopping X_1 and X_2 , respectively. Further calculations at various sets of model parameters have also shown, that the phase diagrams plotted in Figs. 7,8,9 are generic. This suggests that the above choice of model parameters captures the essential physics and does not represent an oversimplification.

In Fig. 7 we present the changes in the stability domain induced by the usage of plaquette Hamiltonians containing no next-nearest neighbor interactions instead of bond Hamiltonians used in¹². The shaded region shows the enlargement of the stability domain of the fully saturated ferromagnetic state. As can be seen from the figure there is a reasonable extension with respect to t_1 . While in the case of bond Hamiltonians X_1 should be very close in magnitude to t_1 in order to reach the lower bound of the stability region, being at $U_{\min} \approx 4$ eV, using plaquette Hamiltonians we have a much broader region for that. The broadening hence implies, that the additionally incorporated correlations really lead to the stabilization of the ordered phase, in our case ferromagnetism.

Since the fully polarized ferromagnetic state at half filling is an exact eigenstate of (7), we have not got any *a priori* restrictions for the values of the interactions. The extensive calculations, however, lead to a simple restriction between $J_{xy}^{(1)}$ and $J_z^{(1)}$. In order to have a ferromagnetic ground state of a model containing spin interactions continuously changing from a Heisenberg-type to a simple Ising-type one, the $-1 < \Delta_1^{XY} \leq 1$ requirement should hold. This means, that the restriction

$$-|J_z^{(1)}| \leq -J_{xy}^{(1)} < |J_z^{(1)}| \quad (21)$$

should always be satisfied. In Fig. 8 the consequence of (21) is illustrated in the U - t_1 cut of the parameter space at $\Delta_1^Z = 1$ and $J_z^{(1)} = -|J_z^{(1)}| < 0$ for various values of Δ_1^{XY} . The size of the stability region is maximal at $\Delta_1^{XY} = 1$ and gradually decreases as Δ_1^{XY} reaches $\Delta_1^{XY} = -1$. Any further decrease of Δ_1^{XY} yields that the fully polarized ferromagnetic state is no longer the ground state of (7). This relation must be obeyed even in the presence of next-nearest neighbor couplings.

In Fig. 9, the effects of nonzero next-nearest neighbor hopping t_2 are illustrated for a fixed set of model parameters, first in the U - t_1 [plot (a), in units of eV] and second in the U - t_2 planes [plot (b), in units of t_1]. In Fig. 9a the dotted line represents the phase boundary in the absence of next-nearest neighbor interactions, while solid, long-dashed, dashed and dotted-dashed lines correspond to phase boundaries in the presence of next-nearest neighbor interactions for various values of t_2 . As can be seen from this plot next-nearest neighbor interactions can help in stabilizing the ferromagnetic state for the chosen set of model parameters as long as t_2/t_1 has a small, positive value. For negative or large positive values of t_2/t_1 , however, the stability domain reduces significantly and stronger Coulomb repulsion is needed for the stabilization. This means e.g., that for a reasonably narrow band ($t_1 \approx 0.4$ eV) at $t_2/t_1 = 0.1$ the required minimal stabilizing Coulomb repulsion is about $U_{\min} \approx 3$ eV, while the same value of U at $t_2/t_1 = -0.25$ is about $U_{\min} \approx 30$ eV, a magnitude larger. Nevertheless, the above range of Coulomb interactions can be considered reasonable for real materials.

In Fig. 9b, the effects of the change in non-interacting dispersion due to the inclusion of next-nearest neighbor hopping are shown for a square (solid line) and for a cubic (dotted line) lattice. The stability domains of ferromagnetism depend on the dimensionality of the underlying lattice and do not coincide. It is interesting to note that the most favorable values of t_2/t_1 , for which the Coulomb interaction takes its minimal value U_{\min} , also depend on dimensionality. The shapes of the stability domains are also of interest: in a well-defined region of t_2/t_1 , U_{\min} changes only by a slight amount, but when the edges of this region are reached, U increases drastically. This feature suggests that inside the stability regions a nonzero next-nearest neighbor hopping via the asymmetric density of states^{13,30} helps (in the presence of other next-nearest neighbor interactions) in stabilizing the fully saturated ferromagnetic state as a ground state of (7), but outside it destabilizes the ferromagnetic ordering. The edges are determined mainly by the dispersions (hence the shape of the particular density of states) and tuned further by other interactions.

It is a well established fact in literature^{4,11,19}, that the inclusion of nearest neighbor ferromagnetic exchange interaction in the pure Hubbard model favors the parallel ordering of electron spins. In Fig. 10, we considered the pure Hubbard model supplemented by next-nearest neighbor hopping t_2 and nearest and next-nearest neighbor exchange interactions J_1 and J_2 , respectively. All the other type of couplings are turned off. As can be seen in the figure, the stability domain of ferromagnetism extends with increasing value of the Coulomb repulsion and in the limit of $U \rightarrow \infty$ fills the whole $J_1, J_2 \leq 0$ quarter of the phase diagram. But the fully polarized ferromagnetic state remains

the ground state of (7) for finite values of U only in the presence of finite values of J_1 and J_2 . Figure 10 also shows that the required minimal values of $|J_2|$ are about an order of magnitude less than the required minimal values of $|J_1|$ and J_2 should be also ferromagnetic in nature, i.e. $J_2 < 0$.

V. CONCLUSIONS

In the present paper, we have studied certain sectors of the ground state phase diagram of the Hubbard model supplemented by nearest and next-nearest neighbor interactions in the thermodynamic limit. The purpose of this study was to clarify to what extent and in which way the inclusion of additional correlations changes the phase boundaries for physically interesting states, the η -pairing state of momentum $P = 0$ or π and the fully polarized ferromagnetic state at half-filling. The new, extended phase boundaries were extracted from the equality of an upper and a lower bound of the ground state energy. Hence they are exact. The additional correlations are introduced by the derivation of the lower bound on elementary plaquettes instead of bonds of the D dimensional hypercubic lattice. Since the applied method requires the investigated state to be an exact eigenstate of the global Hamiltonian, (probably) unphysical restrictions among the model parameters might also emerge. As an example we refer here to Sec. IV A, where the η -pairing states are examined in more detail. Such unphysical restrictions, however, do not occur in the case of the fully saturated ferromagnetic state.

Due to the difficulties that emerged during the analytic diagonalization of the plaquette Hamiltonian, the exact phase boundaries could not be given in closed forms, except in the case of η -pairing of momentum $P = 0$. Instead, the boundaries were illustrated graphically in special cuts of the parameter space of the model under study. The special choice of the cuts, however, does not mean a loss of generality. The phase boundaries presented here are sufficient which means that outside the derived regions the considered state might also be the ground state. By diagonalization of the local Hamiltonians defined on larger clusters of the underlying lattice, these sufficient conditions might be further improved. This improvement of stability regions due to the increase of cluster size addresses a further issue: do the considered ordered phases extend further if larger and larger clusters are chosen, or is there a convergence regarding the location of the phase boundaries? If the latter holds, we would be able to determine the stability domains of various ordered states of (7) also in the limit of $H = h_{\text{cluster}}$ with a simple extrapolation. Based on preliminary results, we believe that any further extension is rapidly decreasing with increasing cluster size. For instance, deriving the lower bounds with the usage of local Hamiltonians defined on clusters of 6 lattice sites instead of plaquettes, the further expansion of the stability regions is about a few percentage, generally 4-5 %.

Considering the effects of more local correlations, which is practically equivalent to the choice of local Hamiltonians defined on larger clusters, it was possible to improve significantly the previously derived rigorous results of^{11,12,24,25} for all the states examined here. In the case of the fully polarized ferromagnetic case this means e.g., that for reasonable values of nearest neighbor interactions the minimal value of the Coulomb repulsion required to stabilize ferromagnetism is predicted by our model to be about 6-12 eV for a relatively broad range of nearest neighbor hopping t_1 (see Fig. 7).

Another goal of the present study was to determine the collective effects of next-nearest neighbor interactions on the stability domains. Using plaquette Hamiltonians the inclusion of next-nearest neighbor interactions could be done in a natural way. To our knowledge, the effects of next-nearest neighbor interactions have not yet been considered rigorously in literature. They have, however, notable effects on the phase diagram. The stability conditions are strongly dependent on them; their effect is either an extension or a shrinking of the stability domain in various sectors of the phase diagram. For instance, in the case of η -pairing of momentum $P = \pi$ the possible maximal value of the Coulomb repulsion U_{max} , up to which the η_π -state remains the ground state of the extended Hubbard model (i.e. the model has a superconducting ground state), is increased from 6 eV to 8-9 eV ($D = 3$) by the inclusion of relatively small next-nearest neighbor interactions (Fig. 6b).

It is also a well-established fact that next-nearest neighbor hopping of single particles, which is characterized by the hopping amplitude t_2 , is important in real materials. The results presented in the previous section are also in good agreement with this fact: they show that t_2 has a characteristic effect on the stability of the fully saturated ferromagnetic state. Even a small ratio of t_2/t_1 , i.e. a small amount of frustration in the dispersion, leads to a considerable change in the phase diagram. The change is mostly a shrinking of stability domain, but for small values of the ratio ($t_2/t_1 \leq 0.15$) the presence of a t_2 helps in stabilizing ferromagnetism (Fig. 9). This is in good agreement with recent DMRG studies taken on $D=1$ dimensional triangular lattice³¹. However, it is interesting to note, that an extension of the ferromagnetic domain occurs always at positive ratios of t_2/t_1 for fixed values of the other parameters.

The Hubbard model supplemented only by exchange interactions J_1 and J_2 has also been investigated. Our finding is in good agreement with the results in Ref.³², i.e. the critical values of nearest and next-nearest exchange interactions to give rise to ferromagnetism approach zero as $U \rightarrow \infty$ in the case of a half-filled band in any dimensions. However,

at finite values of U , J_1 and J_2 should also be finite if the ground state is the fully polarized ferromagnetic state.

In summary, we have established a simple method which allows us to incorporate and to treat the effects of next-nearest neighbor correlations and interactions in an *exact* fashion. We showed that the ground state in the present model at half filling is superconducting or ferromagnetic, depending on the interaction values. The exact phase boundaries of these states for certain sets of model parameters have also been constructed.

VI. ACKNOWLEDGMENTS

The author would like to thank Zs. Gulácsi and E. Müller-Hartmann for their continuous encouragement during the present work. He also thanks A. Schadschneider, G. Uhrig and P. Wurth for valuable discussions and careful reading of the manuscript. The author is gratefully acknowledges financial support of Deutscher Akademischer Austauschdienst (DAAD) and the hospitality of the University of Cologne, Germany.

¹ E.H. Lieb and F.Y. Phys. Rev. Lett. **20**, 1445 (1968).
² W. Metzner and D. Vollhardt, Phys. Rev. Lett. **62**, 324 (1989).
³ E. Müller-Hartmann, Z. Phys. B **74**, 507 (1989); *ibid.* **76**, 211 (1989).
⁴ J.C. Amadon and J.E. Hirsch, Phys. Rev. **B54**, 6364 (1996).
⁵ M. Ulmke, Eur. Phys. J. B **1**, 301 (1998).
⁶ F.H.L. Essler, V.E. Korepin and K. Schoutens, Phys. Rev. Lett. **70**, 73 (1993).
⁷ A.A. Ovchinnikov, J. Phys. **CM6**, 11057 (1994).
⁸ U. Brandt and A. Gieseckus, Phys. Rev. Lett. **68**, 2648 (1992).
⁹ A. Mielke and H. Tasaki, Comm. Mat. Phys. **158**, 341 (1993).
¹⁰ R. Strack and D. Vollhardt, Phys. Rev. Lett. **70**, 2637 (1993).
¹¹ R. Strack and D. Vollhardt, Phys. Rev. Lett. **72**, 3425 (1994).
¹² J. de Boer and A. Schadschneider, Phys. Rev. Lett. **75**, 4298 (1995).
¹³ T. Hanisch, G.S. Uhrig and E. Müller-Hartmann, Phys. Rev. **B56**, 13960 (1997).
¹⁴ H. Tasaki, Phys. Rev. Lett. **75**, 4678 (1995).
¹⁵ R. Hlubina, S. Sorella and F. Guinea, Phys. Rev. Lett. **78**, 1343 (1997).
¹⁶ C. Verdozzi and M. Cini, Phys. Rev. **B51**, 7412 (1995).
¹⁷ J. van den Brink *et al.*, Phys. Rev. Lett. **75**, 4658 (1995).
¹⁸ Zs. Szabo and Zs. Gulácsi, Phil. Mag. **B76**, 911 (1997).
¹⁹ J.E. Hirsch, Phys. Rev. **B56**, 11022 (1997).
²⁰ M. Kollar, R. Strack and D. Vollhardt, Phys. Rev. **B53**, 9225 (1996).
²¹ C.N. Yang, Rev. Mod. Phys. **34**, 694 (1962).
²² C.N. Yang, Phys. Rev. Lett. **63**, 2144 (1989).
²³ S.-Q. Shen and Z.-M. Qiu, Phys. Rev. Lett. **71**, 4238 (1993).
²⁴ J. de Boer, V.E. Korepin and A. Schadschneider, Phys. Rev. Lett. **74**, 789 (1995).
²⁵ A. Montorsi and D.K. Campbell Phys. Rev. **B53**, 5153 (1996).
²⁶ A.A. Aligia and L. Arrachea, Phys. Rev. Lett. **73**, 2240 (1994).
²⁷ A. Schadschneider, Phys. Rev. **B51**, 10386 (1995).
²⁸ J. Hubbard, Proc. R. Soc. London A **276**, 238 (1963).
²⁹ J. Appel, M. Grodzicki and F. Paulsen, Phys. Rev. **B47**, 2812 (1993).
³⁰ J. Wahle *et al.*, cond-mat/9711242 (unpublished).
³¹ R. Arita, Y. Shimoi, K. Kuroki and H. Aoki, Phys. Rev. **B57**, 10609 (1998).
³² J.E. Hirsch J. Appl. Phys. **67**, 4549 (1990).

FIG. 1. An elementary plaquette of the $D = 2$ dimensional square lattice. Solid lines represent different types of nearest neighbor couplings while dashed lines symbolize the next-nearest neighbor ones. In what follows, the local Hamiltonian is defined on this cluster.

FIG. 2. Exact stability region of η -pairing state of momentum $P = 0$ (η_0) at half filling. The shaded region represents the enlargement of the stability domain due to the choice of local Hamiltonian defined on elementary plaquettes (see Fig. 1) of the lattice. All the next-nearest neighbor interactions are kept to be zero.

FIG. 3. Exact stability domains of η -pairing state of momentum $P = \pi$ (η_π) at half filling for two different sets [plot (a): $X_1 = 0.1$ eV, $V_1 = -2$ eV and $J_1 = 0.05$ eV; plot (b): $X_1 = 0.1$ eV, $V_1 = -2$ eV, $J_{xy}^{(1)} = -0.02$ eV and $J_z^{(1)} = -0.015$ eV] of nearest neighbor couplings in the absence of next-nearest neighbor interactions. The shaded regions represent the enlargement of the stability domain due to the choice of the local Hamiltonian defined on plaquettes instead of bonds.

FIG. 4. Effects of correlated hopping X_1 and pair hopping Y_1 on the stability of η -pairing state of momentum $P = \pi$ (η_π). All the next-nearest neighbor interactions are turned off. We note, that beyond a well-defined value of Y_1 the phase boundaries for the cases $X_1 \neq t_1$ and $X_1 = t_1$ coincide.

FIG. 5. Stability domains of η -pairing state of momentum $P = \pi$ (η_π) in $D = 3$ in the presence of various on-site Coulomb repulsions and intersite density-density type (V_1, V_2) interactions. The remaining parameters of model (7) are chosen as follows: $t_2 = -\frac{1}{4}t_1$ and $X_1 = J_1 = J_2 = 0$. Note, that X_2, Y_1 and Y_2 are uniquely fixed via the rigorous restrictions derived earlier in order that (13) be an exact eigenstate. We also note here, that in $D = 2$ similar stability regions emerge.

FIG. 6. Effects of next-nearest neighbor (NNN) couplings on the stability of η -pairing states of momentum P on a two dimensional square lattice. The values of the interaction constants are fixed as follows; plot (a): $P = 0$, $V_1 = -3$ eV, $J_{xy}^{(1)} = \frac{1}{40}$ eV, $J_z^{(1)} = \frac{1}{30}$ eV, $t_2 = \frac{1}{3}t_1$, $V_2 = \frac{1}{3}V_1$ and $J_a^{(2)} = \frac{1}{3}J_a^{(1)}$ ($a = xy, z$); plot (b): $P = \pi$, $V_1 = -2$ eV, $X_1 = 0.5$ eV, $J_{xy}^{(1)} = -\frac{1}{50}$ eV, $J_z^{(1)} = -\frac{1}{40}$ eV, $t_2 = -\frac{1}{3}t_1$, $V_2 = \frac{1}{3}V_1$ and $J_a^{(2)} = \frac{1}{3}J_a^{(1)}$ ($a = xy, z$); plot (c): $P = \pi$, $X_1 = \frac{1}{2}t_1$, $J_1 = -2Y_1$, $t_2 = -\frac{1}{5}t_1$, $Y_2 = \frac{1}{8}Y_1$ and $J_2 = \frac{1}{8}J_1$.

FIG. 7. Exact stability region for the fully saturated ferromagnetic state (FM) at half filling on a D dimensional hypercubic lattice for a certain set of model parameters $X_1 = 0.5$ eV, $V_1 = 2$ eV and $Y_1 = -J_1 = \frac{1}{40}$ eV in the absence of next-nearest neighbor interactions. The shaded region represents the extension of the stability of the fully saturated ferromagnetic state as the ground state of model (7) due to the choice of local Hamiltonian defined on the elementary plaquettes, instead of bonds, of the lattice.

FIG. 8. Stability regions of the fully saturated ferromagnetic state (FM) for various values of Δ_1^{XY} . The stability region is maximal at $\Delta_1^{XY} = 1$ and vanishes for values $\Delta_1^{XY} < -1$. The numerical values of the remaining couplings are the same as in Fig. 7.

FIG. 9. Effects of next-nearest neighbor couplings on the stability of the fully saturated ferromagnetic state (FM) in the t_1 - U and t_2 - U planes, plot (a) and (b), respectively, at half filling. Plot (a) shows the phase boundaries for various ratios of t_2/t_1 , with numerical values of nearest neighbor interactions being the same as in Fig. 7. For this plot the next-nearest neighbor interactions are as follows: $X_2 = 0.08$ eV, $V_2 = \frac{1}{8}V_1$, $Y_2 = \frac{1}{5}Y_1$ and $J_2 = \frac{1}{5}J_1$. In plot (b) all the interaction constants are expressed in units of t_1 instead of units of eV. Above each line the ground state is the fully polarized ferromagnetic state.

FIG. 10. Stability of the fully saturated ferromagnetic state (FM) in the presence of nearest (J_1) and next-nearest (J_2) neighbor exchange coupling at $t_2 = -\frac{1}{10}t_1$. All the other interactions are turned off, i.e. $X_1 = X_2 = V_1 = V_2 = Y_1 = Y_2 = 0$.

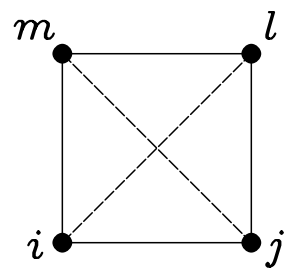


Figure 1
Z. Szabó

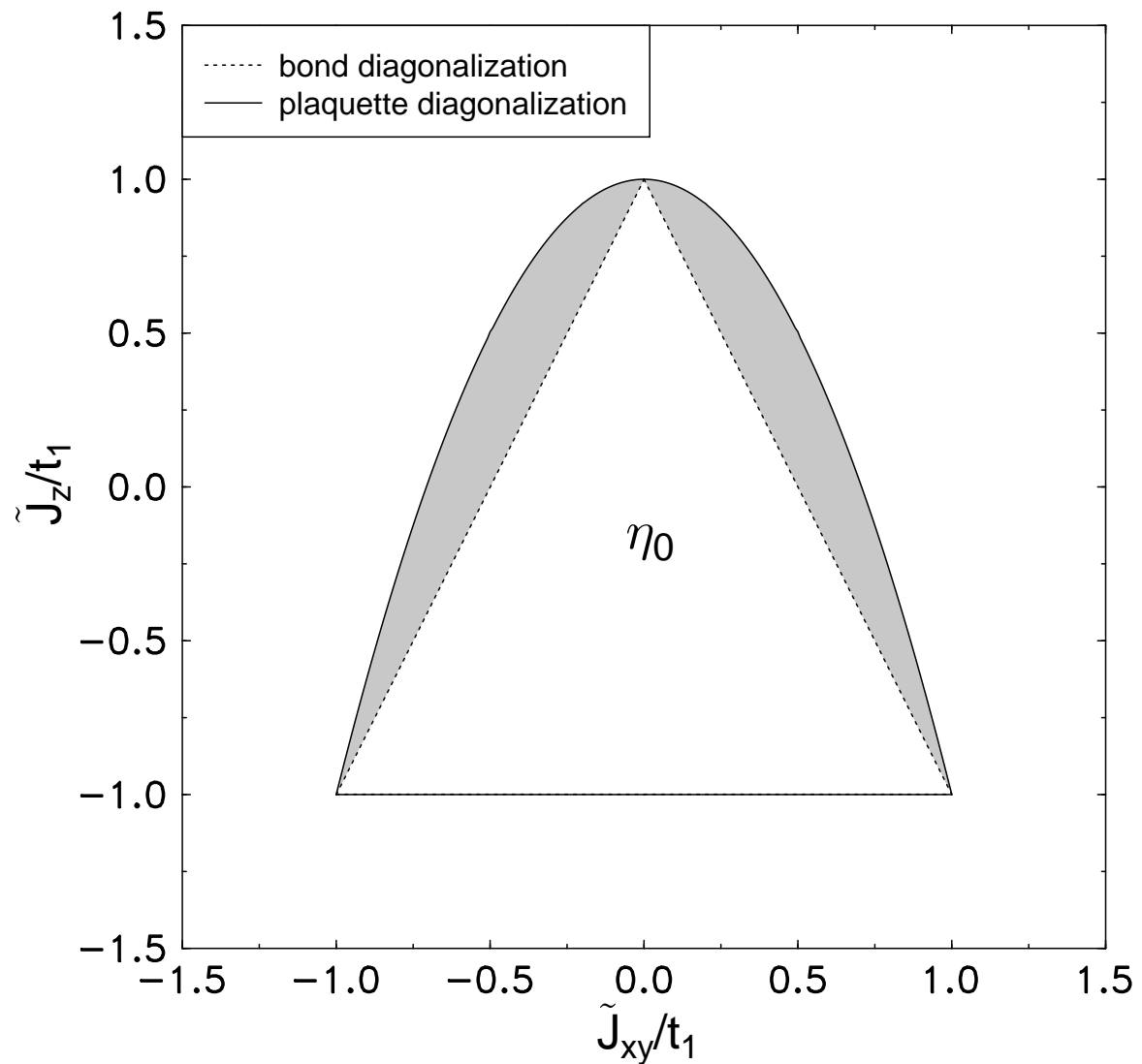


Figure 2

Z. Szabó

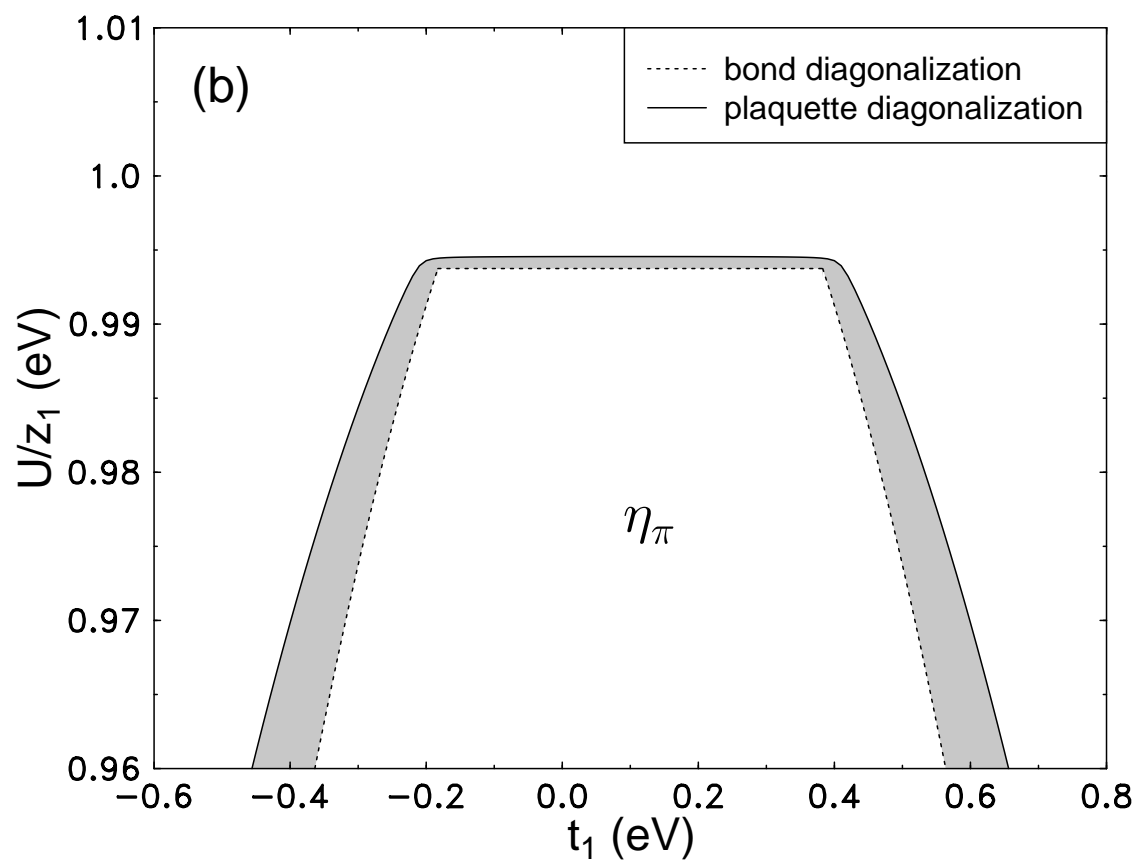
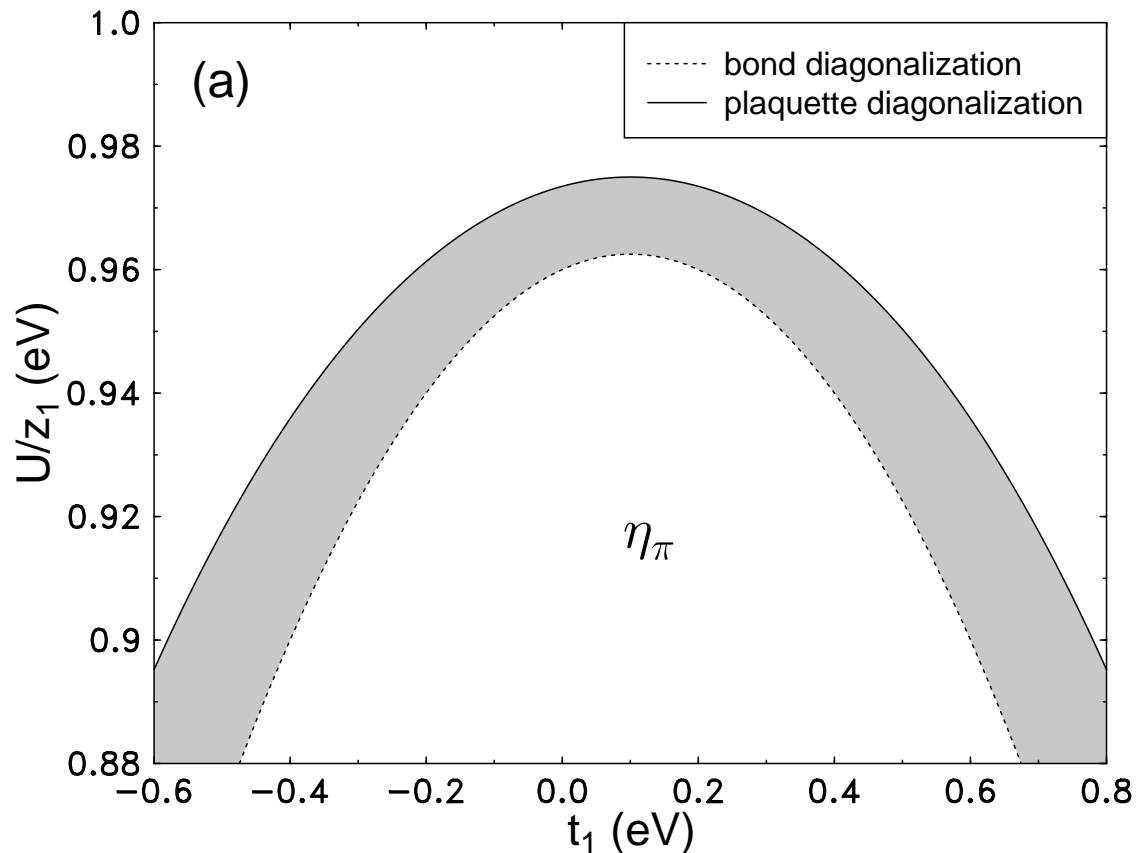


Figure 3

Z. Szabó

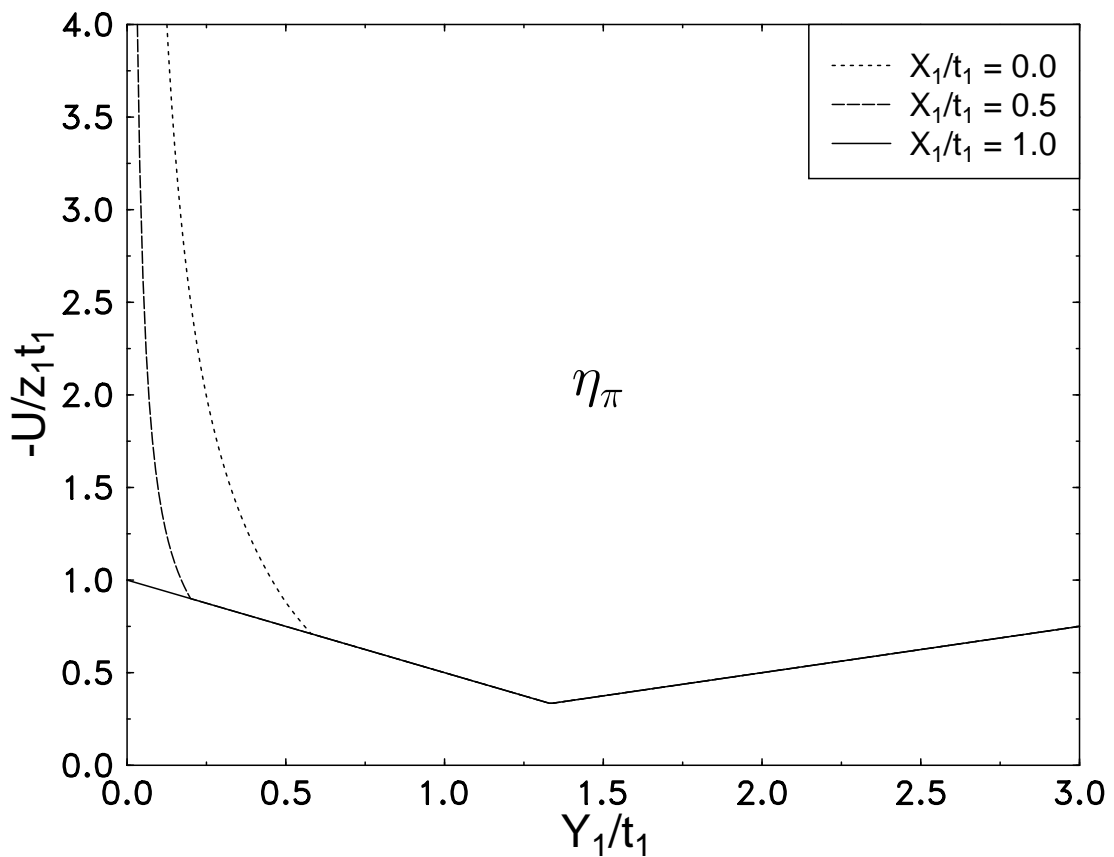


Figure 4

Z. Szabó

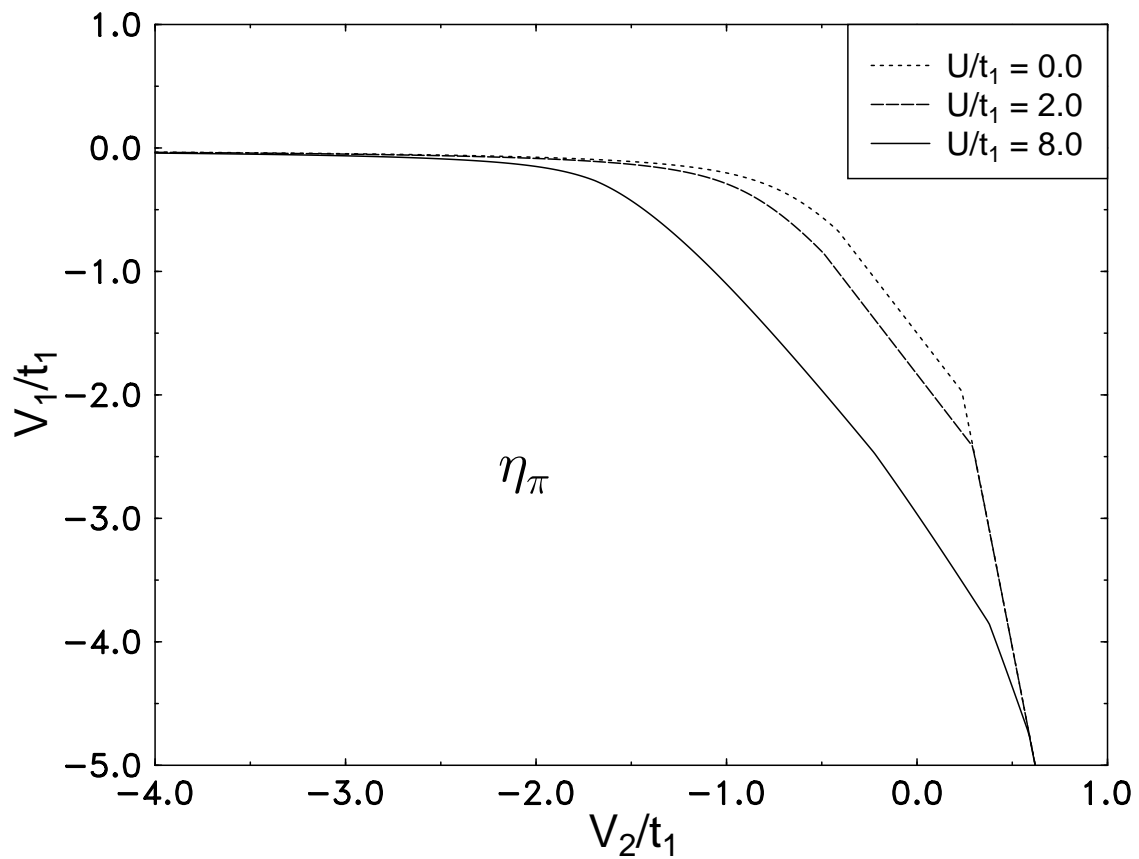


Figure 5

Z. Szabó

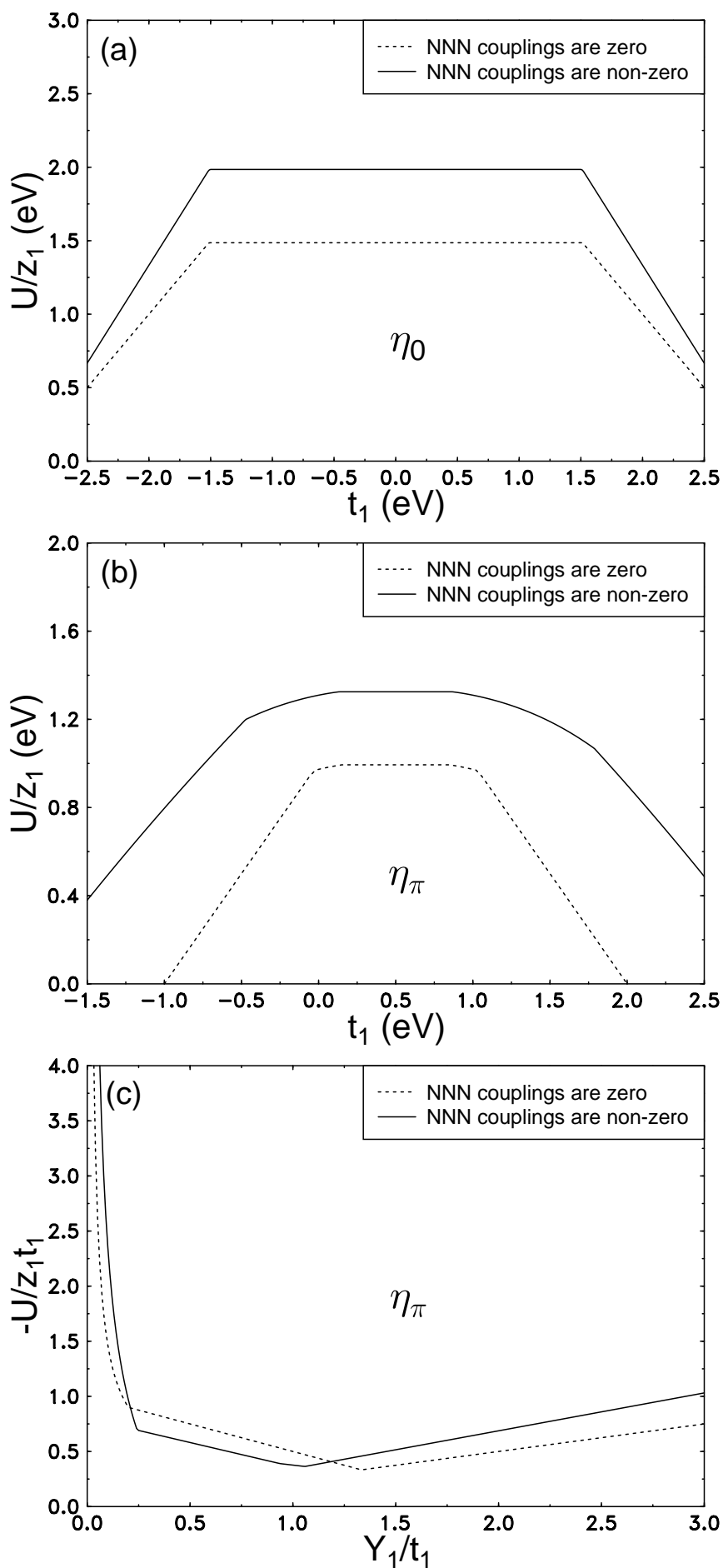


Figure 6

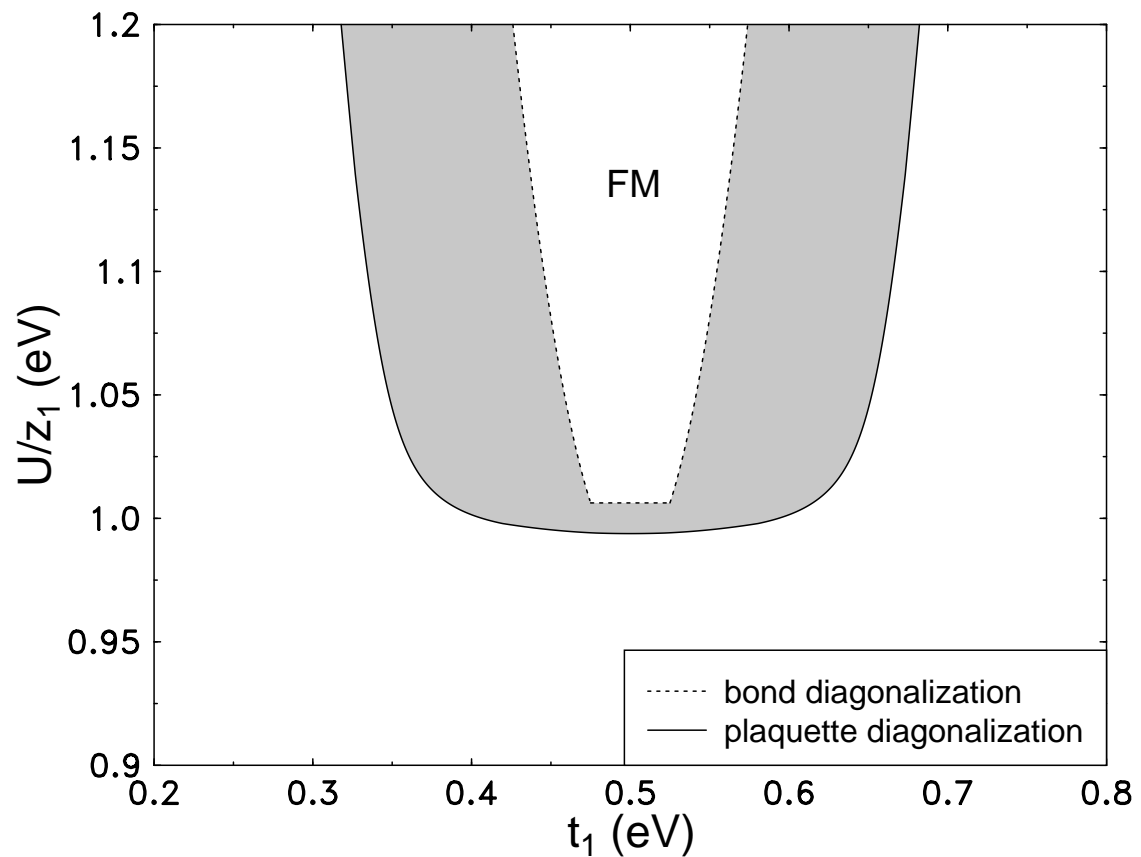


Figure 7

Z. Szabó

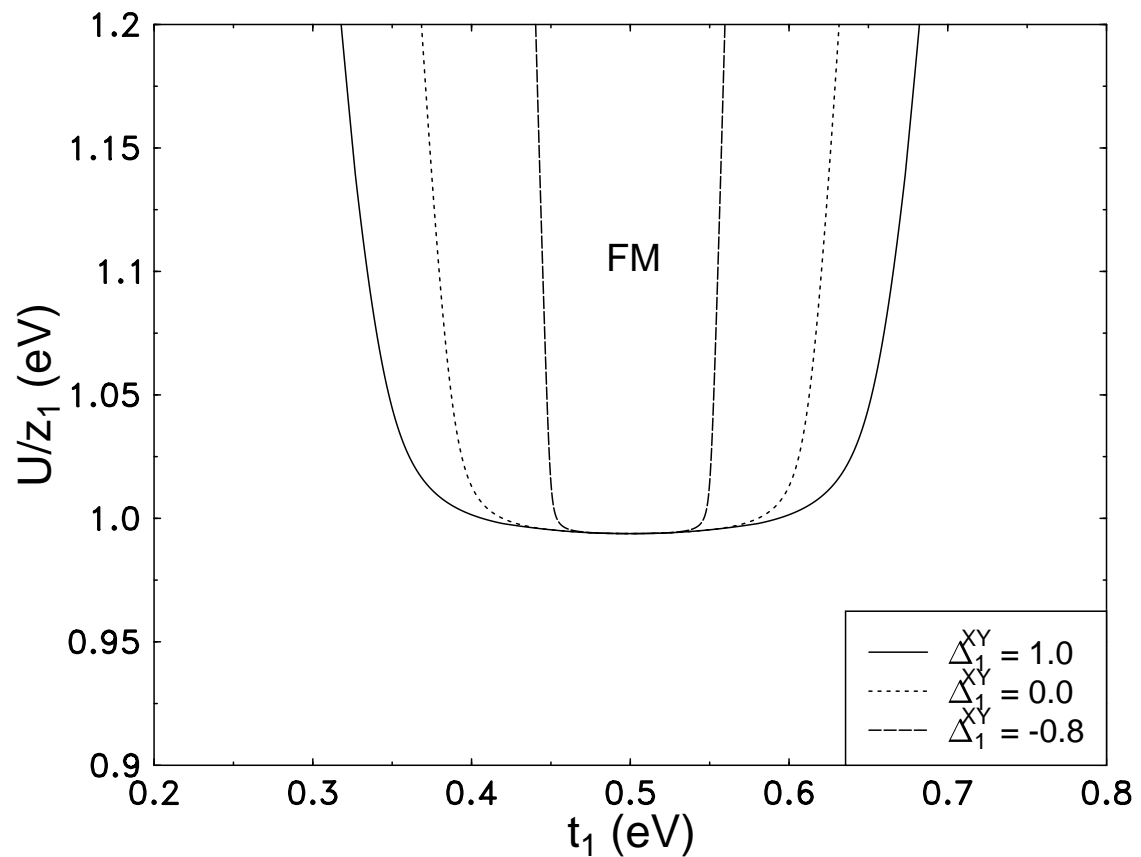


Figure 8

Z. Szabó

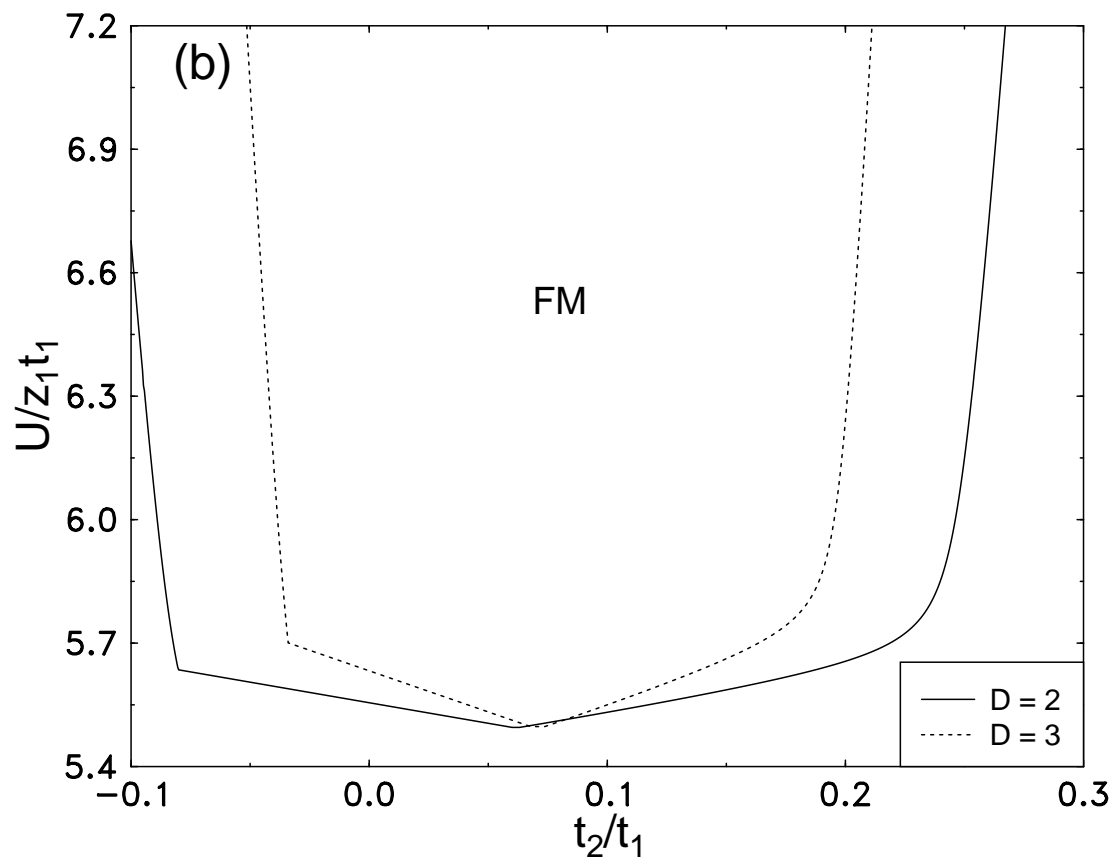
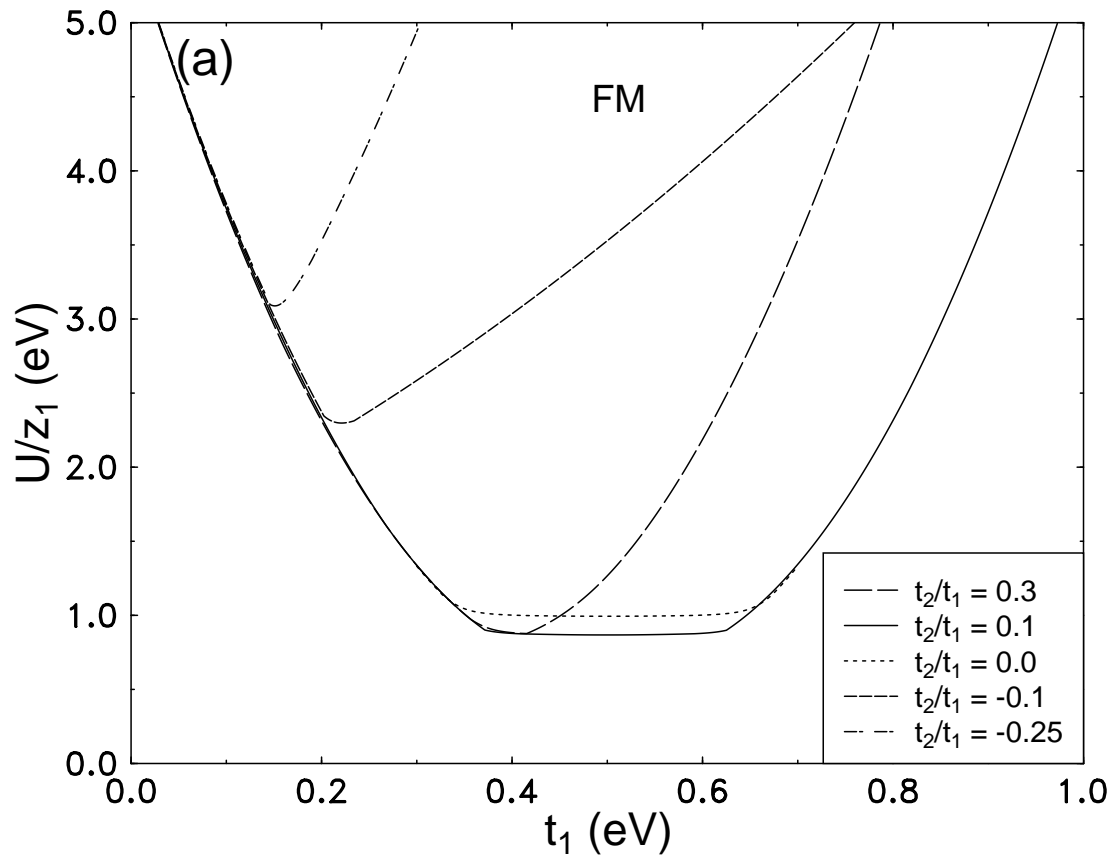


Figure 9

Z. Szabó

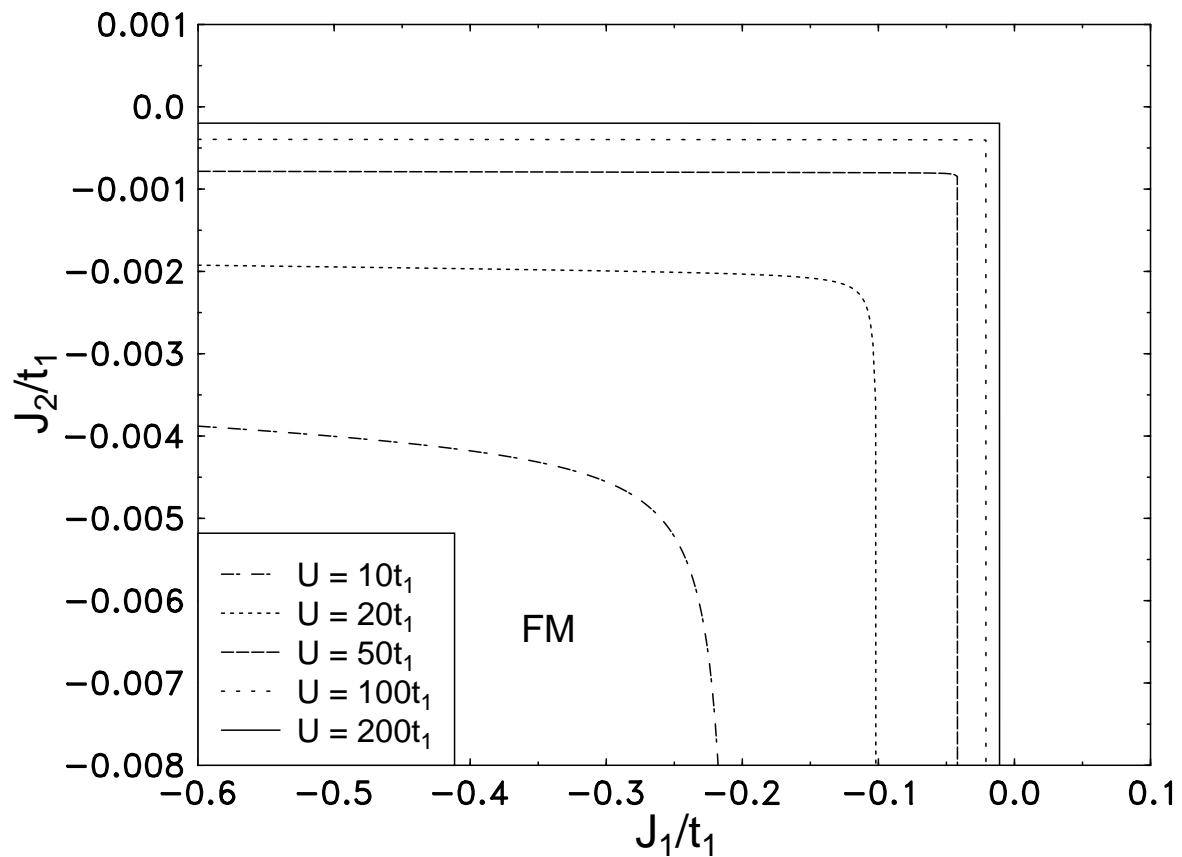


Figure 10

Z. Szabó